Geochimica et Cosmochimica Acta 386 (2024) 84–95

Contents lists available at ScienceDirect

Geochimica et Cosmochimica Acta

journal homepage: www.elsevier.com/locate/gca

The Role of Mafic Intrusions in Producing Alkaline Vent Fluids at the Lost City Hydrothermal Field: Evidence from Stable Potassium Isotopes

Guy N. Evans *, Soisiri Charin, William E. Seyfried Jr., Xin-Yuan Zheng *

Department of Earth and Environmental Sciences, University of Minnesota, Minneapolis, MN, 55455, USA

ARTICLE INFO

Associate editor: Eva Stüeken

Keywords:
Potassium isotopes
Seafloor hydrothermal
Ultramafic
Serpentine
Alkaline vent

ABSTRACT

The alkaline, H_2-rich vent fluids of the Lost City Hydrothermal Field (LCHF) have generally been attributed to serpentinization of tectonically uplifted mantle peridotite. However, elevated concentrations of highly incompatible and fluid mobile trace alkali metals, Rb and Cs, indicate reaction with relatively unaltered mafic components (Seyfried et al., 2015). Here, we present high-precision stable-K isotope analyses of LCHF vent fluids, which provide new constraints on source-rock lithology and support more quantitative estimates of fluid:rock ratio, providing a new constraint on heat and mass transfer processes. We find that $\delta^{41}K$ values of LCHF vent fluids (0.03–0.07 ‰) are distinct from local seawater (0.13 ± 0.02 ‰). In combination with near-seawater concentrations of K (10.4 ± 0.1 mmol/kg), these data are incompatible with hydrothermal alteration of peridotite alone, which is highly depleted in K. Instead, K-isotope and concentration data are consistent with hydrothermal alteration of mafic rocks (e.g., gabbro or diabase) at a fluid:rock ratio of 6–26, a range that agrees well with Rb, Cs, and $^{87}Sr/^{86}Sr$-based estimates of fluid:rock ratio, updated here to reflect derivation from mafic source rocks.

Geochemical modeling of hydrothermal fluid-rock reactions indicates that LCHF vent fluids can be effectively reproduced by a two-stage reaction in which seawater initially reacts at 200–300 °C with mafic rocks at in a fluid:rock ratio of ~ 10 —as constrained by the above isotopic and trace-element systematics— and subsequently reacts with peridotite at a fluid:rock ratio of ~ 30 at roughly the same temperature, pressure conditions. We also note that LCHF vent fluids are ~ 2 % depleted in Cl compared to seawater, which may reflect admixture of a vapor component derived from ongoing phase separation at higher (> 450 °C) temperatures. We thus propose that the LCHF represents waning-stage hydrothermal activity initiated by a discrete off-axis mafic intrusion that has subsequently cooled to intermediate temperatures conducive to olivine hydrolysis and production of alkaline vent fluids. In this interpretation, alkaline H_2-rich vent fields occupy a narrow thermal window in the expected evolution of hydrothermal activity associated with episodic off-axis mafic intrusions into tectonically exposed ultramafic host rocks and are thus likely to be rare on the modern seafloor.

1. Introduction

Crustal extension along slow-spreading mid-ocean ridges —estimated to characterize ~ 50 % of the modern ridge axis and ~ 23 % of the modern seafloor at full spreading rates < 40 mm/yr (Cannat et al., 2010)— is accommodated by interspersed volcanism and tectonic exposure of lower crustal and mantle rocks along long-lived, low-angle detachment faults (Mutter and Karson, 1992; Dick et al., 2003). Tectonic movement along these low-angle detachment faults can form off-axis domal massifs known as oceanic core complexes (Cann et al., 1997; Tucholke et al., 1998; MacLeod et al., 2009).

Seafloor hydrothermal vents associated with oceanic core complexes exhibit diverse fluid chemistry ranging from high-temperature, highly acidic, H_2-rich fluids that exhibit high Fe concentrations and high Fe:S ratios, such as those discovered at the Logatchev (Batuyev et al., 1994; Krasnov et al., 1995; Schmidt et al., 2007), Rainbow (Fouquet et al., 1998; Charlou et al., 2002; Douville et al., 2002), Ashadze (Beltenev et al., 2003), Niebelungen (Devey et al., 2005; Melchert et al., 2008; Schmidt et al., 2011), Semenov (Beltenev et al., 2007), and Irinovskoe (Beltenev et al., 2012) vent fields on the Mid-Atlantic Ridge, to lower-temperature (< 116 °C), alkaline, H_2-rich, Si-, Fe-, and sulfide-poor vent fluids discovered at the Lost City Hydrothermal Field (LCHF),

* Corresponding authors.
E-mail addresses: gevans@umn.edu (G.N. Evans), zhengxy@umn.edu (X.-Y. Zheng).

https://doi.org/10.1016/j.gca.2024.08.030
Received 15 April 2024; Accepted 31 August 2024
Available online 4 September 2024

also on the Mid-Atlantic Ridge (Kelley et al., 2001; 2005). High-temperature, acidic, Si-, H_2–, Fe-, and sulfide-rich vent fluids have also been discovered at the Kairei and Edmond vent fields on the Central Indian Ridge (Gallant and Von Damm, 2006), and the Longqi Vent Field on the Southwest Indian Ridge (Tao et al., 2021). The < 226 °C, moderately acidic, H_2– and Si-rich, Fe-poor vent fluids discovered at the Von Damm Hydrothermal Field on the Mid-Cayman Rise represent another distinct vent fluid type (McDermott, 2015; McDermott et al., 2015). Based on the occurrence of similar carbonate-brucite vent structures, the weakly venting Old City site on the Southwest Indian Ridge (Lecouevre et al., 2021) and the inactive (fossil) Ghost City and Clamstone sites on the Rainbow Massif near the Rainbow Vent Field (Lartaud et al., 2010; 2011) are proposed to have been formed by processes similar to those currently active at the LCHF.

Despite these diverse and, in some cases, divergent chemical characteristics, vent fluids collected from all these sites have been attributed to hydrothermal alteration of ultramafic and mafic rocks, in various proportions to each other and to seawater-derived fluids, and at different reaction temperatures. For example, the acidic, metal-rich fluids of the Rainbow Vent Field have been attributed to high-temperature (> 400 °C) alteration of mixed ultramafic and mafic rocks (Douville et al., 2002; Allen and Seyfried, 2003; Seyfried et al., 2011; Debret et al., 2018), whereas the contrasting alkaline, metal-poor fluids of the LCHF have been attributed to lower-temperature (200–300 °C) alteration of predominantly ultramafic rocks (Kelley et al., 2001; 2005), with minor mafic influence (Seyfried et al., 2015). It has also been proposed that many of these diverse fluid types are linked by geologic processes associated with different stages in the development of oceanic core complexes, exhumation of lower crustal and mantle rocks, and extensive fluid flow along the bounding detachment faults (McCaig et al., 2007).

This study focuses on alkaline, H_2– and CH_4 –rich vent fluids collected at the LCHF, which have typically been attributed to serpentinization of mantle peridotite, tectonically uplifted to form the Atlantis Massif (e.g., Kelley et al., 2001; Kelley et al., 2005; Seyfried et al., 2015). This interpretation is supported by the results of numerous hydrothermal experiments involving olivine serpentinization reactions, which invariably produce alkaline, H_2-rich fluids at moderate < 350 °C reaction temperatures (Seyfried and Dibble, 1980; Janecky and Seyfried, 1986; Berndt et al., 1996; Seyfried et al., 2007; McCollom et al., 2016; McCollom et al., 2020). Also supporting this interpretation are extensive seafloor sampling (Blackman et al., 2002; Boschi et al., 2006; Karson et al., 2006), shallow (< 20 m) drilling (IODP Expedition 357; Früh-Green et al., 2017; 2018; Rouméjon et al., 2018; Liebmann et al., 2018), and recent deep (1268 m) drilling (IODP Expedition 399, McCaig et al., 2024; Lissenberg et al., 2024) of the underlying south wall of the Atlantis Massif, which comprises variably serpentinized peridotite, primarily harzburgite and dunite, and subordinate (~30 %) mafic rocks, including gabbro, diabase, and minor basalt (Blackman et al., 2002; Boschi et al., 2006; Karson et al., 2006; Rouméjon et al., 2018; McCaig et al., 2024; Lissenberg et al., 2024). Recent sampling of the water column surrounding the Atlantis Massif and fluids emanating from nascent drill holes provides evidence for decentralized hydrogen production attributed to ongoing serpentinization within the Atlantis Massif, albeit distinct from LCHF fluids, which contain elevated concentrations of both H_2 and CH_4 (Lang et al., 2021).

Elevated concentrations of Rb and Cs, in contrast, have long been interpreted to indicate subsurface reaction with plagioclase, presumably within mafic rocks (Seyfried et al., 2015). Moreover, detailed petrologic studies of Atlantis Massif seafloor- and drill core samples report Si-metasomatism of serpentinized peridotite in the form of amphibole + chlorite ± talc veins and talc mineralization, and Ca-metasomatism of altered gabbro indicative of prior stages of hydrothermal activity involving focused flows of high-temperature, low-pH, sulfur containing mafic-derived fluids (Boschi et al., 2006; 2008; Rouméjon et al, 2018; Liebmann et al., 2018; Whattam et al., 2022a, 2022b). Cross-cutting relations and diabase dikes and sheets exhibiting chilled margins and semi-brittle deformation textures indicate that at least some of this high-temperature alteration postdates exhumation of the massif and pervasive serpentinization of the peridotite at shallow depths (Rouméjon et al., 2018; Liebman et al., 2018). The relationship between past circulation of these inferred acidic, mafic-derived hydrothermal fluids within the Atlantis Massif and the alkaline fluids currently venting at the LCHF remains unclear.

In this study, we use high-precision stable K isotope analyses as a new tool to investigate the subsurface processes that generate LCHF vent fluids. These stable K isotope data are considered in the context of previous data on LCHF vent fluid chemistry and host-rock lithology and complementary geochemical modeling. Vent fluids collected from the LCHF contain near-seawater concentrations of K (K = 10.3–10.5 mmol/kg; Seyfried et al., 2015), which has been previously assumed to derive entirely from seawater (e.g., Allen and Seyfried, 2004). However, hydrothermal reaction of plagioclase, as indicated by elevated fluid Rb and Cs concentrations (Seyfried et al., 2015), potentially mobilizes rock-derived K with a K isotope signature distinct from seawater. Thus, K isotope analyses of LCHF vent fluids promise to offer new insights into the hydrothermal processes underlying the LCHF.

Results of previous stable-K isotope studies have indicated that seawater (Hille et al., 2019) and oceanic crust (Wang et al., 2016) exhibit homogeneous $\delta^{41}K$ values. Analyses of mid-ocean ridge basalt and ocean island basalt indicate that $\delta^{41}K$ values are unaffected by partial melting or fractional crystallization (Tuller-Ross, 2019a, 2019b) and reflect homogeneous $\delta^{41}K$ values in mantle source rocks (Hu et al., 2021). However, the $\delta^{41}K$ value of seawater ($\delta^{41}K_{NIST3141a}$ = 0.12 ‰ ± 0.07 ‰ relative to the NIST 3141a standard; Wang et al., 2020) contrasts with that of oceanic crust ($\delta^{41}K_{NIST3141a}$ = -0.45 ± 0.05 ‰; Wang et al., 2016) and estimated mantle values ($\delta^{41}K_{NIST3141a}$ = -0.42 ± 0.08 ‰; Hu et al., 2021). The detectability of this natural isotopic contrast is enhanced by increased analytical precision enabled by recent advances in K stable-isotope techniques (e.g., Zheng et al., 2022a). On the other hand, the relative mass balance of K in seawater (10.1 mmol/kg) and average mid-ocean ridge basalt (MORB) (K_2O = 0.14 wt%; K = 30 mmol/kg, Gale et al., 2013) is considerably more balanced than that of other elements (e.g., Li, Sr) conventionally analyzed to differentiate seawater- and crustal contributions to hydrothermal fluids. Together, these facts indicate that K isotopes are potentially sensitive indicators of hydrothermal reactions that inherently offer a more balanced perspective on seawater- and rock-derived components than isotopic systems dominated by rock or seawater. Previous studies reported that $\delta^{41}K$ values of high-temperature acidic seafloor vent fluids typically span the range between MORB and seawater, providing support for fluid K isotopes in tracing fluid-rock interactions (Zheng et al, 2022b; Ramos et al., 2022). These studies primarily focused on global K cycles and did not pursue detailed investigations of processes specific to individual vent fields and did not report data on alkaline LCHF vent fluids.

2. Geologic Setting

The Lost City Hydrothermal Field (30° 07' N, 42° 07' W, 750–900 m below sea level) is located 15 km west of the Mid-Atlantic Ridge spreading axis on the south wall of the Atlantis Massif, an oceanic core complex located at the inside corner of the Mid-Atlantic Ridge and the Atlantis Fracture Zone (Kelley et al., 2001). The Atlantis Massif can be subdivided into three geologically distinct zones: the eastern Hanging Wall, the Central Dome, and the Southern Ridge, which hosts the LCHF (Fig. 1). The eastern Hanging Wall is a volcanic terrain thought to be a

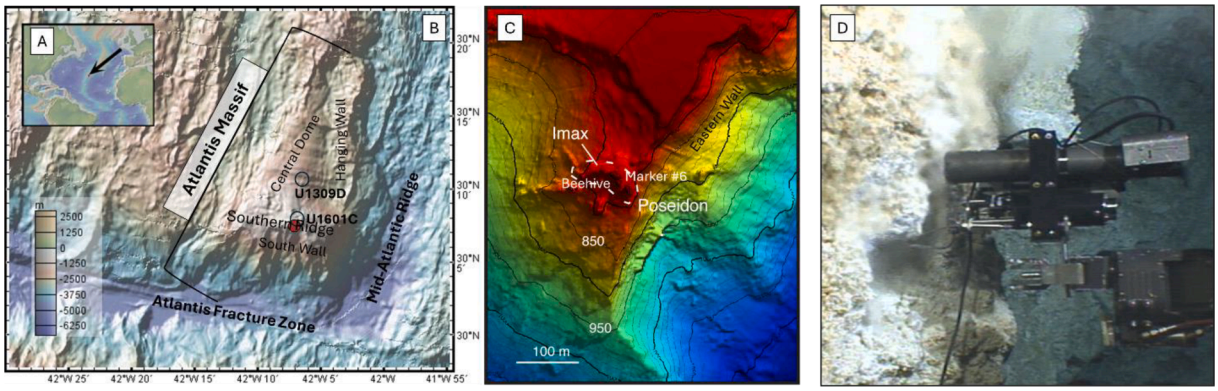

Fig. 1. (A) Inset showing location of the Atlantis Massif in the Atlantic Ocean and (B) bathymetric map of the Atlantis Massif. Red circle indicates the location of Lost City Hydrothermal Field (LCHF) on the Atlantis Massif. Open circles indicate the locations of IODP drilling stations, U1309D (Expedition 305, Ildefonse et al., 2006) and U1601C (Expedition 399). (C) Detailed bathymetric map of LCHF from Kelley et al. (2005) showing the location of the "Poseidon" vent structure. (D) Sampling at Beehive vent on the Poseidon vent structure (Seyfried et al., 2015). Background bathymetric map in (A) produced using GeoMapApp (https://www.geomapapp.org) and bathymetry from Global Multi-Resolution Tomography, ver. 4.2.0. (Ryan et al., 2009). Bathymetric data in (C) are from Kelley et al. (2005). Geologic interpretations in (A) and (C) follow those of Kelley et al. (2005), Blackman et al. (2011), and Lang et al. (2021).

detached segment of the detachment-fault hanging wall. The Central Dome, which was the target of IODP Expeditions 304 and 305 (Ildefonse et al., 2006; Blackman et al., 2006; 2011) comprises dominantly gabbroic sequences, as evidenced by deep oceanic drilling to 1415 m below seafloor during IODP Expedition 305 (Blackman et al., 2006), deepened to 1498 m during Expedition 399 (McCaig et al., 2024), and seismic tomography (Canales et al., 2008; Henig et al., 2012). Morphologically offset from the Central Dome, the Southern Ridge comprises variably serpentinized peridotite and subordinate (~30 %) mafic, predominantly gabbroic, rocks, as evidenced by seafloor sampling (Kelley et al., 2001; 2005; Blackman et al., 2002; Boschi et al., 2006; Karson et al, 2006), shallow (< 20 m) drilling (IODP Expedition 357; Früh-Green et al., 2018; Rouméjon et al., 2018; Liebmann et al., 2018), and deep (1268 m) drilling (IODP Expedition 399, McCaig et al., 2024; Lissenberg et al., 2024). The morphologic offset between the Central Dome and Southern Ridge has also been proposed to represent tectonic faulting (Karson et al., 2006) and a resultant hydrologic discontinuity (Titarenko and McCaig, 2016). Seismic tomography and comparative drilling results confirm that the morphologic offset observed at the seafloor continues to deeper depths and that the Southern Ridge is geologically distinct from the Central Dome, though a high seismic velocity zone similar to the Central Dome is also present in the eastern Southern Ridge (Canales et al., 2008; Henig et al., 2012). This high velocity zone has been proposed to represent predominantly gabbroic lithology, compositionally similar but possibly morphologically separate from that underlying the Central Dome, that may have been influential in the geodynamic development and current morphology of the Atlantis Massif (Henig et al., 2012).

Active venting at the LCHF occurs on the south wall of the Southern Ridge of the Atlantis Massif (Fig. 1C), along a > 200 m east–west lineament at 800–850 m water depth (Kelley et al., 2001; 2005). Vent fluids from the main "Poseidon" vent structure are alkaline (pH (at 25 °C) = 10.1–10.5), H_2-rich (H_2 = 9.9–11.5 mmol/kg) and enriched in Ca (25.3–27.5 mmol/kg), Li (41–44 μmol/kg), Rb (2.7–2.8 μmol/kg), and Cs (13–20 nmol/kg) relative to seawater (Kelley et al., 2001; Seyfried et al., 2015; Aquino et al., 2022). More recently, additional vents have been discovered at 855–870 m water depth (Lang et al., 2021). The chemistry of these more recently discovered vent fluids is attributed to a multi-stage evolution of a common source fluid variably modified by mixing with seawater and microbially mediated sulfate reduction prior to venting (Aquino et al., 2022). The focus of this study is on the origin of this source fluid, which is best represented at the seafloor by fluids emanating from the "Poseidon" vent structure, especially the "Beehive" and "Marker #6" vents (Seyfried et al., 2015; Aquino et al., 2022), and the relationship of this source fluid to underlying fluid-rock reactions.

3. Methods

3.1. Sample Collection

Samples of LCHF vent fluids and bottom seawater were originally collected in 2008 from the Beehive (91–116 °C) and Marker #6 (53–78 °C) vents using isobaric gastight samplers (Seewald et al., 2002) deployed on the Jason 2 remotely operated vehicle (KNOX1RR, *R/V Roger Revelle*) (Seyfried et al., 2015). Elemental and isotopic analyses were performed on archived acidified aliquots of these samples stored in the original LDPE sample bottles at the University of Minnesota.

3.2. Elemental Analyses

Elemental analyses were conducted using a triple quadrupole inductively coupled plasma mass spectrometer (Thermo Fisher Scientific iCAP TQ, Waltham, MA, USA) at the University of Minnesota. Fluid samples were diluted 100 × in 2 % HNO_3 prepared from trace metal grade 70 % HNO_3 (RICCA Chemical, Arlington, TX, USA) and 18.2 MΩ•cm deionized water and analyzed by method of standard addition against NIST-traceable single- and multi-element standards (SPEX CertiPrep, Metuchen, NJ, USA) and Sc, Y, Ir in-line internal standards. Comparison of these recent analyses with those published in Seyfried et al. (2015) indicate water loss ranging from 0–50 % over the ~ 14 years of storage with most samples indicating 10–20 % water loss (Supplemental Table S1). Such water loss is insufficient to induce mineral (halite or sylvite) precipitation and element ratios remain conserved, typically exhibiting < 10 % difference compared to ratios calculated from published results in Seyfried et al. (2015). For the purposes of this study, the originally published concentration data of Seyfried et al. (2015) were maintained.

3.3. Potassium Isotope Analyses

Potassium isotope analyses of LCHF vent fluids and local bottom seawater were conducted at the University of Minnesota following the method of Zheng et al. (2022a). Accordingly, a ~ 150 μl aliquot from each sample was first evaporated completely in a Teflon beaker on a hot plate at ~ 120 °C. After cooling down, 400 μl of 0.4 M HCl was added to redissolve each sample, followed by ion-exchange chromatographic separation that purified K from matrix elements. Three reference materials, including a natural seawater sample collected from the South

China Sea and two USGS rock standards (AVG-2a and BCR-2), were processed and analyzed in the same way as unknown samples.

A column separation using Bio-Rad AG 50 W-X8 cation exchange resin (H^+ form, 200–400 mesh) was used in this study. Resin was packed in 2 ml Poly-Prep columns. Samples were loaded onto columns in 400 µl 0.4 M HCl. Sodium was eliminated by passing 23 ml 0.4 M HCl through column, and K was then quantitatively recovered in another 28 ml 0.4 M HCl. Other major cations, such as Mg and Ca, were retained by the resin. Potassium cuts were evaporated and then processed through columns a second time using fresh resin and the same elution protocol. Purified K samples were dissolved in 2 % HNO_3 prior to the K isotope measurement. Optima grade acids, or distilled acids of comparable purity, and ultrapure Milli-Q water (18.2 MΩ•cm) were used throughout sample preparation. The total procedural K blank is estimated to be < 20 ng, which is negligible compared to the typical amount of K processed in a sample (> 100 µg).

Stable K isotopes were analyzed by a multi-collector inductively coupled plasma mass spectrometer (MC-ICP-MS, "Sapphire" from Nu Instruments) at the University of Minnesota. Sample solution was introduced into the instrument by an Apex Omega HF desolvating unit and a ~ 100 µl/min PFA nebulizer. This instrument is equipped with a hexapole collision cell, and the K isotope data reported here were collected using the collision cell mode with helium (He) and hydrogen (H_2) as collision/reaction gases. The use of the collision cell removed argon and argon hydride interferences to a negligible level and, consequently, high precision $^{41}K/^{39}K$ analysis was achieved at low mass resolution and a normal RF power of 1300 W. Samples were analyzed by a sample–standard bracketing protocol where NIST SRM 3141a was used as the bracketing standard. All data in this study are reported against the NIST 3141a scale. Typically, a solution K concentration of ~ 200 ppb was used during the analysis, yielding > 200 V intensity on ^{39}K. The large ^{39}K signal was collected on a Faraday cup with a 10^{10}-ohm resistor. Each sample was analyzed at least 4 times. The long-term reproducibility of our $^{41}K/^{39}K$ measurement is estimated to be 0.05 ‰ (2SD), based on repeated analyses of seawater and USGS rock standards (Table 1).

3.4. Modeling Potassium Isotope Systematics

Previous laboratory experiments (Seyfried et al., 1979) and field studies (Wheat et al., 2000; Hulme and Wheat, 2019) indicate that hydrothermal fluids lose K during low-temperature (< 150 °C) recharge reactions and gain rock-derived K at higher temperatures. To model these processes and quantitatively interpret vent fluid $\delta^{41}K$ data, we employ a two-box fluid-rock interaction model in which a mass of fluid chemically and isotopically equilibrates with an incrementally introduced mass of rock at sequential low-temperature (box 1) and high-temperature (box 2) conditions. A similar modeling approach has been previously used to study other isotope systematics, such as oxygen and boron isotopes, in hydrothermal systems (e.g., Bowers and Taylor, 1985; Magenheim et al., 1995).

3.4.1. Model derivation

Within each box, a certain mass of fluid, F, reacts with a certain mass of rock R, iteratively introduced. The mass of rock introduced at each interval is dR. Potassium (K) mass balance dictates that:

$$F[K]_f^i + R[K]_r^i + dR[K]_r^o = F[K]_f^{i+1} + (R+dR)[K]_r^{i+1} \quad (1)$$

where $[K]_f^i$ is the concentration of K in the fluid at interval i, $[K]_r^i$ is the concentration of K in the rock, also at interval i, and $[K]_r^0$ is the initial K concentration of fresh rock. Simultaneously, K isotope mass balance dictates that:

$$F\delta^{41}K_f^i + R\delta^{41}K_r^i + dR\delta^{41}K_r^0 = F\delta^{41}K_f^{i+1} + (R+dR)\delta^{41}K_r^{i+1} \quad (2)$$

where $\delta^{41}K_f^i$ is the $\delta^{41}K$ value of fluid at interval i and $\delta^{41}K_r^i$ is the $\delta^{41}K$ value of rock, also at interval i; $\delta^{41}K_r^0$ is the $\delta^{41}K$ value of fresh rock. Throughout this process, K partitions according to a constant partition coefficient, expressed by the formula:

$$D_K = \frac{[K]_f^i}{[K]_r^i} \quad (3)$$

where D_K is the K partition coefficient. Isotope equilibrium between K isotopes is also maintained such that:

$$\Delta^{41}K_{f-r} = \delta^{41}K_f^i - \delta^{41}K_r^i \quad (4)$$

where $\Delta^{41}K_{f-r}$ is the equilibrium fractionation between fluid and rock. The solution sets $[[K]_f^i, \delta^{41}K_f^i]$ of these equations for the fluid are defined by:

$$[K]_f^i = \frac{[K]_r^0}{D_k} - \left(\frac{[K]_r^0}{D_K} - [K]_f^0\right) exp\left(\frac{-D_K}{\frac{F}{R}}\right) \quad (5)$$

and

$$\delta^{41}K_f^i = \left(\delta^{41}K_r^0 + \Delta^{41}K_{f-r}\right) - \left(\left(\delta^{41}K_r^0 + \Delta^{41}K_{f-r}\right) - \delta^{41}K_f^0\right) exp\left(\frac{-D_K}{\frac{F}{R}}\right) \quad (6)$$

Importantly, these two formulas are linked by the common term:

Table 1
Analyses of $\delta^{41}K$ in vent fluids from Beehive (BH) Marker #6 (M6) vents, local bottom seawater, and standards. Data for Mg, Cl, and K are from Seyfried et al. (2015).

Sample		Mg mmol/kg	Cl mmol/kg	K mmol/kg	Mg/K mol/mol	Measured $\delta^{41}K$ (‰) AVG	95 % C.I.	n	Endmember $\delta^{41}K$ (‰) AVG	2SD	2SD
Seawater		53.3	554	10.3	5.17	0.13	0.02	5	–-	–-	0.02
J2-360-CGTR	BH	3.6	542	10.5	0.34	0.04	0.03	5	0.03	0.05	0.04
J2-360-IGT2	BH	1.9	542	10.5	0.18	0.05	0.03	5	0.05	0.04	0.04
J2-361-IGT5	BH	1.4	541	10.5	0.13	0.06	0.03	5	0.06	0.05	0.05
J2-361-IGT6	BH	1.1	543	10.4	0.11	0.04	0.02	5	0.04	0.04	0.03
J2-361-IGTB	BH	6.6	543	10.5	0.63	0.08	0.03	5	0.07	0.05	0.04
J2-361-CGTWu	BH	2.4	543	10.3	0.23	0.03	0.01	5	0.03	0.02	0.02
J2-362-IGT2	M6	1.6	541	10.5	0.15	0.05	0.02	5	0.05	0.03	0.03
J2-362-IGT4	M6	1.3	541	10.5	0.12	0.04	0.02	5	0.04	0.03	0.03
Standards											
AVG-2a						−0.45	0.02	8			
BCR-2						−0.44	0.01	27			
South China Sea Seawater						0.13	0.01	62			

$$exp\left(\frac{-D_K}{\frac{F}{R}}\right) \quad (7)$$

Projected onto the $[K]_f^i, \delta^{41}K_f^i$ plane, solution sets $[[K]_f^i, \delta^{41}K_f^i]$ trace linear trajectories in that extend from $[[K]_f^0, \delta^{41}K_f^0]$ at initial conditions, when $\frac{F}{R}$ is infinitely high, toward the theoretical endpoint $[\frac{[K]_r^0}{D_k}, \delta^{41}K_r^0 + \Delta^{41}K_{f-r}]$, when $\frac{F}{R} = 0$, which represents fluid in equilibrium with an infinite rock reservoir. The K concentration and isotope composition of fresh rock is the same for both low- and high-temperature boxes. However, the partitioning coefficient, D_K, and the isotope fractionation factor, $\Delta^{41}K_{f-r}$, are temperature-dependent, albeit held constant within each box. Thus, fluids evolve toward different rock-dominated endpoints under low- and high-temperature conditions.

The K and K-isotope evolution of LCHF vent fluids is modeled as starting from an initial seawater composition toward the low-temperature endpoint ending at an unknown "altered seawater" composition. This altered seawater then evolves toward the high-temperature endpoint, passing through the composition of Lost City vent fluids. If a solution exists, a unique altered seawater composition may be determined corresponding to a unique set of low-temperature and high-temperature fluid:rock ratios. Solutions for altered seawater compositions were solved using code written in the MATLAB coding language, included as a Supplementary File.

3.4.2. Model Parameters

The chemical and isotopic compositions of fluids in the proposed two-box model are controlled by the parameters $[K]_r^0$, D_K, $\delta^{41}K_r^0$ and $\Delta^{41}K_{f-r}$. The K concentration of mafic rocks is estimated to be 20 mmol/kg, based on oceanic drill cores of the Atlantis Massif that recover diabase and basalt of depleted mid-ocean ridge basalt (D-MORB) compositions (Godard et al., 2009) and the average D-MORB composition (K_2O = 0.096 wt%; K = 20 mmol/kg) of Gale et al. (2013). The K concentration of peridotite is estimated to be < 1 mmol/kg, based on analyses of mantle harzburgite by Wang and Ionov (2023). The initial $\delta^{41}K$ value of rock is set at −0.45 ‰ (Wang et al., 2016) and the initial $\delta^{41}K$ value of seawater is set at 0.12 ‰ (Wang et al., 2020).

Estimates of K partition coefficients at low- and high-temperatures are based on the experiments of Seyfried et al. (1979) and Evans et al. (2023) (Table 2). Low-temperature K isotope fractionation factors are based on Liu et al. (2021), who estimate a K isotope fractionation factor of α = 0.9995 ($\Delta^{41}K$ = 0.5 ‰) between aqueous fluid and low temperature altered oceanic crust. Because these estimates are based on isotope analyses of digested samples or whole rocks, the mineralogical controls on these isotope fractionation factors are poorly known. For the purposes of modeling, we explore low-temperature $\Delta^{41}K_{f-r}$ values of 0.0–0.5 ‰. Recent data on $\delta^{41}K$ values in sheeted dike samples indicate that high-temperature fluid-rock reaction leads to preferential extraction of light K into evolved hydrothermal fluids (Li et al., 2024). For modeling purposes, we thereby explore high-temperature $\Delta^{41}K_{f-r}$ values of 0.0–0.2 ‰.

Table 2
Results of basalt alteration experiments used to derive low-temperature and high-temperature K partition coefficients.

	Unit	Method	Seyfried et al. (1979)	Evans et al. (2023)
Temperature	°C		70	350
Pressure	bar		1	500
		Initial Condition		
Fluid	g	gravimetric	200	40
Fluid K	mmol/kg	gravimetric	10.1	0
Rock	g	gravimetric	20	40
Rock K	mmol/kg	ICP-MS	19	28.4
Total K	mmol	calculated	2.40	1.14
		Final Condition		
Fluid K	mmol/kg	ICP-MS	9.5	25.7
Fluid K	mmol	calculated	1.9	1.0
Rock K	mmol	calculated	0.50	0.11
Rock K	mmol/kg	calculated	25.1	2.7
Partition Coefficient (D_K)		calculated	2.65	0.11

3.5. Geochemical Modeling

Geochemical modeling of fluid-rock reactions and predicted fluid compositions and alteration mineral assemblages was performed using the React module of Geochemists' Workbench (GWB, Bethke and Yeakel, 2014) and a 250-bar database generated using PyGeochemCalc (Awolayo and Tutolo, 2022) with solid solutions enabled and clay mineral solid solutions disabled. The relevant input, output, and database files are included as Supplementary Material.

To model hydrothermal reactions, an initial fluid of roughly seawater composition is first reacted with a mafic mineral assemblage comprising 60 wt% plagioclase (An_{70} = $Ca_{0.7}Na_{0.3}Al_{1.7}Si_{2.3}O_8$), 30 wt% clinopyroxene ($Di_{80}Hed_{20}$ = $CaMg_{0.8}Fe_{0.2}Si_2O_6$) and 10 wt% olivine ($Fo_{80}$ = $Mg_{1.6}Fe_{0.4}SiO_4$) and subsequently reacts with a peridotite mineral assemblage comprising 80 wt% olivine (Fo_{90} = $Mg_{1.8}Fe_{0.2}SiO_4$), 15 wt% orthopyroxene (En_{90} = $Mg_{0.9}Fe_{0.1}SiO_3$), and 5 wt% clinopyroxene ($Di_{90}Hed_{10}$ = $CaMg_{0.9}Fe_{0.1}Si_2O_6$). The initial fluid is based on the chemical composition of seawater and contains seawater concentrations of Mg, sulfate, Ca, and Si. To match K-isotope systematics during low-temperature hydrothermal reaction derived from K-isotope modeling (Section 4.1.), the K concentration is lowered from seawater value of ~ 10 mmol/kg to ~ 9 mmol/kg. The chlorinity of the input fluid is adjusted to match Lost City vent fluid values, and Na is adjusted for charge balance.

Modeled reaction fluids are transferred from mafic to peridotite reactions using the "pickup" function, which copies the calculated elemental composition of model output fluid to the model input. Fluid pH at 25 °C is determined using the same "pickup" function and numerically modeling conductive cooling to 25 °C with all mineral precipitation reactions suppressed.

Model chemical compositions of minerals are based on electron microprobe analyses of olivine, orthopyroxene, plagioclase, and clinopyroxene in samples from the U1309D drill core by Drouin et al. (2009). Clinopyroxene is only a minor component of Atlantis Massif peridotite (McCaig et al., 2024), but is included in the model to account both for the presence of clinopyroxene, as well as the Ca component of orthopyroxene, for which appropriate solid solution data are not available. Endmember LCHF vent fluids contain ~ 3 mmol/kg sulfate despite high H_2 concentrations (Seyfried et al., 2015). Accordingly, the sulfide-sulfate redox reaction is decoupled in the model.

In the absence of appropriate thermodynamic data for K substitution into plagioclase solid solution, the K component of mafic rocks is represented by 5.5 g K-feldspar per 1 kg rock (K_2O = 0.096 wt%), consistent with the D-MORB composition of Gale et al. (2013) and data indicating that plagioclase is the predominant mineral host of K in oceanic crust that has undergone high-temperature hydrothermal alteration (Li et al., 2024). The inclusion of K-feldspar in the model is intended to approximate the effect of K as a component of plagioclase solid solution, not the presence of K-feldspar as a modal mineral.

Reactions are modeled at 250 °C and 250 bar, following previous estimates of LCHF reaction temperatures (Allen and Seyfried, 2004; Blackman et al., 2006; Reeves et al., 2012; Seyfried et al., 2015) and application of the 113 °C/km thermal gradient observed during drilling of the Atlantis Massif Central Dome (Blackman et al., 2014).

Conceptually, these reactions occur ~ 1.7 km below the 0.8 km-deep seafloor. Input, output, and database files for an alternate 350-bar model are included in Supplementary Material.

4. Results

4.1. Potassium Isotope Analyses

Lost City vent fluids exhibit a narrow range of measured $\delta^{41}K$ values between 0.03 ‰ ± 0.03 ‰ and 0.08 ‰ ± 0.03 ‰ (Table 1) Local bottom seawater has a $\delta^{41}K$ value of 0.13 ± 0.02 ‰ (Table 1), confirming the K isotope homogeneity of global seawater (Hille et al., 2019; Wang et al., 2020). To account for seawater contamination during sampling, measured vent fluid compositions were extrapolated to a zero-Mg/K endmember (Zheng et al., 2022b; Ramos et al., 2022). Because of the low Mg concentrations inherent to the samples, this correction is < 0.01 ‰. Endmember $\delta^{41}K$ values range between 0.03 ± 0.05 ‰ and 0.07 ± 0.05 ‰, with an average of 0.05 ± 0.02 ‰ (Table 1). The variability between individual LCHF vent fluid samples is thus within the calculated error of the analyses, which, along with other chemical parameters, which similarly extrapolate to consistent endmember values (Seyfried et al., 2015), indicates that individual fluid samples are effectively replicates of the same vent fluid. The $\delta^{41}K$ values of LCHF vent fluids are resolvably lower than seawater ($\delta^{41}K$=0.13 ± 0.02 ‰) and substantially higher than MORB ($\delta^{41}K$=-0.45 ‰), thus revealing a clear imprint of fluid-rock reactions despite near-seawater K concentrations.

Modeling of K isotope systematics indicates that the observed $\delta^{41}K$ and K concentrations in LCHF vent fluids cannot be simultaneously explained by hydrothermal reaction of peridotite alone because fluid–peridotite reaction that gives rise to fluid $\delta^{41}K$ similar to our measurements could only produce fluid K concentrations less than 10 mmol/kg (Fig. 2). Alternatively, the K concentration and isotope composition of LCHF vent fluids can be reproduced by fluids reacting with mafic rocks of D-MORB composition (Fig. 2). Calculated fluid:rock ratios consistent with this scenario range from 6 to 26 (Table 3). These results

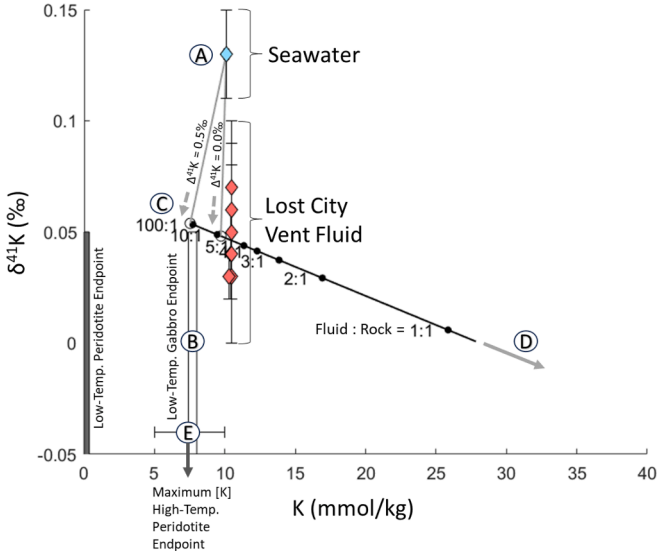

Fig. 2. Modeled evolution of K concentrations and isotope values. Original seawater (A) evolves toward low-temperature gabbro endpoint (B), becoming altered seawater (C) designated by open circles. Subsequent evolution toward high-temperature gabbro endpoint (D) results in Lost City vent fluids at a fluid:rock ratio of 6–26. Labeled fluid:rock ratios correspond to low-temperature fractionation factor of $\Delta^{41}K_{f-r}$ = 0.5 ‰ and a resulting fluid:rock ratio of 6.5. Notably, fluid evolution toward the high-temperature peridotite endpoint (E) would result in K depletion relative to seawater, opposite what is observed.

Table 3
Potassium-isotope derived estimates of high-temperature fluid:rock ratios calculated by assuming different K isotope fractionation factors ($\Delta^{41}K_{f\text{-}r}$) during low-temperature (columns) and high-temperature (rows, labeled in first column) fluid-rock reactions.

		Δ^{41}K Low-Temperature (‰)					
		0.0	0.1	0.2	0.3	0.4	0.5
High-Temperature Δ^{41}K (‰)	0.0	25.7	23.2	20.3	16.7	12.3	6.5
	0.1	25.6	23.2	20.2	16.6	12.2	6.4
	0.2	25.5	23.1	20.1	16.6	12.1	6.3

imply that low-temperature hydrothermal alteration causes a slight depletion in the K concentration of circulating fluids (7.5–9.7 mmol/kg) relative to seawater (10.1 mmol/kg).

4.2. Alternative Estimates of Fluid:Rock Ratio

LCHF vent fluids are enriched in trace alkali metals, Rb and Cs (Seyfried et al., 2015). Assuming complete extraction, and D-MORB composition of underlying rocks, a fluid:rock ratio of 8.6 is estimated based on Rb and 7.7 for Cs (Table 4). Water:rock ratios previously estimated from Sr isotope data for LCHF also fall in this range (2–4, Foustoukos et al., 2008; 3–13, Aquino et al., 2022). Using this same method (Berndt et al., 1988) and D-MORB Sr concentrations (Sr = 111 mg/kg = 1.27 mmol/kg, Gale et al., 2013) results in a calculated water/rock ratio of 27 (Table 4; see Supplement for details and caveats).

4.3. Geochemical Modeling

Modeled reaction of seawater with mafic rocks (60 wt% plagioclase, 30 wt% clinopyroxene, 10 wt% olivine) at 250 °C, 250 bar at a fluid:rock ratio of 10 —broadly consistent with the above fluid:rock ratio estimates— is predicted to produce a mildly acidic (pH at 25 °C = 5.9), Na-depleted (Na = 420 mmol/kg), Ca-enriched (Ca = 57.7 mmol/kg), Si-enriched (Si = 2.4 mmol/kg) fluid (Table 5). The predicted alteration mineral assemblage comprises 38 wt% secondary clinopyroxene, 41 wt % paragonite, 16 wt% vermiculite, 4 wt% andradite, and 3 wt% anhydrite. If the precipitation of Na-bearing alteration minerals, paragonite and analcime, is suppressed, estimated Na (Na = 490 mmol/kg) and Ca (Ca = 24.4 mmol/kg) concentrations closely reassemble those of LCHF vent fluids and the predicted alteration mineral assemblage comprises 27 wt% vermiculite, 23 wt% montmorillonite, 23 wt% epidote, 21 wt% prehnite, 3.5 wt% anhydrite, and 2 wt% secondary clinopyroxene (Table 5). Subsequent reaction with peridotite (80 wt% olivine, 15 wt% orthopyroxene, 5 wt% clinopyroxene) produces fluids with pH and H_2 concentrations (pH (at 25 °C) = 11.0; H_2 = 10.7 mmol/kg) consistent with those of LCHF vent fluids (pH (at 25 °C) = 10.6; H_2 = 10.8 mmol/kg) at a fluid:rock ratio of ~ 30. The predicted alteration mineral

Table 4
Fluid:rock ratios based on LCHF vent fluids and depleted mid-ocean ridge basalt (D-MORB, Gale et al., 2013). Rock-derived Rb and Cs concentrations are based on elemental enrichments relative to seawater. Fluid:rock ratios are then calculated by assuming that Rb and Cs are quantitatively partitioned into the fluid (e.g., Von Damm et al., 1985). Fluid:rock ratios based on Sr and $^{87}Sr/^{86}Sr$ are based on the analyses of Foustoukos et al. (2008) and Aquino et al. (2022) using the methods of Berndt et al. (1988) and additional calculations performed here that account for higher Sr concentrations in mafic rocks (see Supplement).

		Seawater	Lost City Vent Fluid	Rock-Derived	D-MORB	Fluid:Rock Ratio (g_{fluid}/g_{rock})
K	mmol/kg	10.1	10.5	–-	20	6–26
Rb	μmol/kg	1.4	2.8	1.4	12	8.6
Cs	nmol/kg	2.3	17	15	113	7.7
Sr	μmol/kg	82	92	38	1267	27
$^{87}Sr/^{86}Sr$		0.70917	0.7065		0.70269	

Table 5
Results of geochemical modeling indicate that LCHF vent fluid compositions can be effectively reproduced by two-stage hydrothermal reaction involving (1) mafic and (2) ultramafic rocks. Geochemical modeling was performed using the React module of Geochemists' Workbench (Bethke and Yeakel, 2014) and a 250-bar database created using PyGeochemCalc (Awolayo and Tutolo, 2022). Inclusion of K-feldspar in the model is intended to approximate the effect of a K component of plagioclase solid solution, for which appropriate thermodynamic data are currently lacking. Sulfide-sulfate redox was decoupled. supp. = precipitation suppressed; mont. = montmorrilionite.

Parameter	unit	Initial Fluid	Stage 1 Mafic		Stage 1 Mafic supp: paragonite, analcime		Stage 2 Ultramafic		LCHF Vent Fluids
Pressure	bar	250		250		250		250	70
Temperature	C	250		250		250		250	< 116
Mineral Reactants			Total (g)	100	Total (g)	100	Total (g)	31	
	g		An_{70}	60	An_{70}	60	Fo_{90}	25	
	g		$Di_{80}Hed_{20}$	30	$Di_{80}Hed_{20}$	30	En_{90}	4.7	
	g		Fo_{80}	10	Fo_{80}	10	$Di_{90}Hed_{10}$	1.6	
	g		K-feldspar	0.4	K-feldspar	0.4			
Fluid:Rock	g:g			10		10		32	
Fluid	g	1000		1000		1000		1000	1000
pH	in situ	7.2		6.0		6.0		7.3	6.9
pH	at 25 °C	8.0		5.9		8.1		11.0	10.6
H_2O	g	969		966		965		961	969
Cl	mmol/kg	541		543		543		545	541
Na	mmol/kg	464		420		490		490	494
Ca	mmol/kg	10		57.7		24.4		27.5	27.4
K	mmol/kg	9		10.5		10.5		10.5	10.5
H_2	mmol/kg	0		0.05		0.05		10.7	10.8
SO_4^{2-}	mmol/kg	28		2.9		8.8		8.8	3.2
H_2S	mmol/kg	–-		–-		–-		–-	< 0.2
Mg	mmol/kg	53		0.01		0.0		0.0	0.0
Si	μmol/kg	24		2376		3043		4.8	< 73
Al	μmol/kg	1		2.3		5.2		5.2	–-
Fe	μmol/kg	0.001		0.5		0.0		0.0	< 18.4
Mineral Products			Total (g)	105	Total (g)	107	Total (g)	36	
	g		paragonite	43	vermiculite	29	lizardite	31	
	g		$Di_{80}Hed_{20}$	33	prehnite	23	magnetite	3.0	
	g		$Di_{70}Hed_{30}$	5	mont.	25	brucite	0.4	
	g		vermiculite	17	epidote	25	monticellite	0.6	
	g		andradite	4	anhydrite	3			
	g		anhydrite	3	$Di_{90}Hed_{10}$	2			

assemblage for this second stage of reaction comprises 89 wt% lizardite, 8.6 wt% magnetite, 1.7 wt% monticellite, 1.1 wt% brucite (Table 5). Calculated fluid chemistry for reactions at 350 bar are broadly similar to those produced at 250 bar. At 350 bar, the Stage-1 alteration mineral assemblage is predicted to include andradite and secondary clinopyroxene instead of montmorillonite and epidote.

5. Discussion

Stable K isotope data provide a new constraint on the origin of LCHF vent fluids, supplementing previous data on vent fluid pH, major-ion and dissolved volatile (H_2, H_2S, CO_2, CH_4) concentrations (Kelley et al., 2001; 2005; Foustoukos et al., 2008; Seyfried et al., 2015; Aquino et al., 2022), B concentrations, ^{11}B, $\delta^{18}O$, and $^{87}Sr/^{86}Sr$ isotope values (Foustoukos et al., 2008), alkali metal concentrations (Seyfried et al., 2015), and methane isotopologues (Wang et al., 2018). Other important aspects of LCHF vent fluids previously reported include the concentrations and isotopic signatures of short chain hydrocarbons (Proskrowski et al., 2006) and organic acids (Lang et al., 2010), which are influential in understanding abiotic organic synthesis processes at the LCHF and geologic sources of energy and organic carbon for associated microbial communities (Lang et al., 2018). Likewise influential are studies of pervasive shallow serpentinization (Boschi et al., 2008; Delacour et al., 2008), sulfur cycling (Liebmann et al., 2018), and decentralized H_2 production (Lang et al., 2021). Such processes have been proposed to support an extensive subsurface biosphere at Atlantis Massif, while also demonstrating that pervasive serpentinization, near quantitative sulfate reduction, and decentralized H_2 production are distinct from LCHF venting and occur at much higher integrated water–rock ratios (typically > 100) (Boschi et al., 2008; Delacour et al., 2008; Liebmann et al., 2018). Here, we examine the implications of K isotope data for determining the origin of the LCHF source fluid in the context of underlying fluid-rock reactions and previously reported geochemical data.

5.1. Potassium Isotope Systematics

Potassium isotope analyses reveal a rock-derived component of K in LCHF vent fluids. In the absence of isotopic data, LCHF vent fluid K was assumed to be entirely derived from seawater (e.g., Allen and Seyfried, 2004). This newly recognized rock-derived K component of LCHF vent fluids and previously recognized enrichment in Rb and Cs point to involvement of relatively unaltered mafic rocks (e.g., gabbro or diabase), which contain elevated concentrations of K and other alkali metals, in the generation of LCHF vent fluids. In contrast, hydrothermally altered gabbro, metadolerite, and serpentinized peridotite (harzburgite and dunite) collected from the south wall of the Atlantis Massif are highly depleted in K and other trace alkali metals (Früh-Green et al., 2018). The lack of K enrichment in fluids derived from hydrothermal alteration of peridotite has also been confirmed experimentally (Seyfried and Dibble, 1979; Grozeva et al., 2017). Stable K isotope data additionally constrain estimated fluid:rock ratios to relatively high values (6–26), whereas enrichments in alkali metal concentrations could be alternatively accommodated by very low fluid:rock ratios and mantle compositions (e.g., fluid:rock = 0.6–0.9, Seyfried et al., 2015).

5.2. Geochemical Modeling

Geochemical modeling results indicate that LCHF vent fluids can be effectively reproduced by a two-stage reaction involving (Stage 1) mafic and (Stage 2) ultramafic rocks. Magnesium depletion, Ca enrichment, and alkali metal enrichment occur in the first stage reaction of seawater with mafic rocks, while the alkaline, H_2-rich, (Si-poor) fluid chemistry characteristic of LCHF vent fluids develops in the second stage of reaction with peridotite. Throughout these reactions, temperature plays an

important role, as experimental studies indicate that rates of olivine hydrolysis are maximized at 200–300 °C (McCollom et al., 2016), which coincides with the estimated temperature range of LCHF fluid-rock reactions (Allen and Seyfried, 2004; Blackman et al., 2008; Reeves et al., 2012; Seyfried et al., 2015; Wang et al., 2018). Thus, comparatively little peridotite is needed to produce alkaline, H_2-rich vent fluids at these optimal temperatures. Models predict that alteration mineral assemblages following Stage 1 comprise various clay minerals and prehnite, whereas alteration mineral assemblages following Stage 2 comprise serpentine and magnetite. These alteration mineral assemblages are broadly similar to those recovered from drilling of the south wall, where static alteration of gabbroic rocks includes replacement of plagioclase by secondary plagioclase, chlorite, prehnite, and zeolite, replacement of pyroxene by amphibole, talc, chlorite and clay minerals, and replacement of olivine by amphibole, talc, serpentine, magnetite, clay minerals (McCaig et al., 2024). Relatively abundant serpentine-magnetite veins are also reported (McCaig et al., 2024).

To summarize, accurate reproduction of LCHF vent fluids in all previously reported chemical aspects requires hydrothermal alteration of previously unaltered mafic rocks (e.g., gabbro or diabase) comprising plagioclase and clinopyroxene, and additional reaction with olivine. Incompatible fluid-mobile elements, K, Rb, and Cs, are available in late-stage mafic intrusions, but not in abyssal peridotite or lower crustal gabbro previously subjected to hydrothermal alteration and fluid flow. From the perspective of fluid chemistry alone, the requisite olivine may be present in ultramafic wall rocks or intrinsic to the mafic intrusion. However, a two-stage model involving hydrothermal reaction of seawater and mafic rocks and subsequent reaction with peridotite better fits reported alteration mineralogy and results of recent drilling that has recovered peridotite containing abundant relict olivine from the south wall of the Atlantis Massif (McCaig et al., 2024; Lissenberg et al., 2024). While this two-stage model is necessarily a simplification of the true Atlantis Massif petrology, where numerous cm- to m-scale gabbroic intrusions occur in variably serpentinized peridotite (Lissenberg et al., 2024), we believe that this model best captures the essential geochemical reactions leading to the development of LCHF vent fluids.

5.3. Linkages between the LCHF and Off-Axis Mafic Intrusions

Previous studies have emphasized the role of peridotite serpentinization in generating the alkaline, H_2-rich vent fluids at LCHF (Kelley et al., 2001; 2005; Foustoukos et al., 2008; Seyfried et al., 2015; Aquino et al., 2022). Mafic intrusions, which have been implicated to support Si-metasomatism earlier in the geologic history of the Atlantis Massif (Früh-Green et al., 2018; Rouméjon et al., 2018; Liebmann et al., 2018), have been generally perceived as being incidental to actively venting fluids, even as some mafic-derived components of these vent fluids have been explicitly (Rb, Cs, Si) or implicitly (Ca, Sr) recognized (Foustoukos et al., 2008; Seyfried et al., 2015; Aquino et al., 2022). Additionally, several studies have long implicated a role for mafic intrusions in providing the heat necessary to drive hydrothermal circulation, albeit as one of several possibilities (e.g., Allen and Seyfried, 2004; Seyfried et al., 2015).

Based on the analysis of our K isotope data and complementary geochemical modeling results, we propose that LCHF vent fluids are derived from off-axis intrusions of relatively unaltered mafic rock (e.g., gabbro or diabase) into olivine-rich mantle peridotite. Such off-axis intrusions inherently provide the external heat necessary to achieve estimated subsurface reaction temperatures of 200 ± 50 °C (Allen and Seyfried, 2004; Foustoukos et al., 2007; Reeves et al., 2012; Seyfried et al., 2015) or 270 $^{+140}/_{-68}$ °C (Wang et al., 2018). Moreover, mafic rocks of essentially D-MORB composition result in consistent fluid:rock ratio estimates across multiple trace element (Rb, Cs) and isotopic methods ($\delta^{41}K$, $^{87}Sr/^{86}Sr$), as well as multicomponent fluid-rock reaction models (Tables 4, 5). Alternative models that do not invoke magmatic heat sources instead require deep (~8 km) circulation of hydrothermal fluids and contrasting geothermal gradients beneath the Southern Ridge and Central Dome (Titarenko and McCaig, 2017) or extremely low fluid flux (e.g., 0.08 kg/s, Lowell, 2017), which is at odds with direct observation of extensive seafloor venting.

To summarize, we propose that LCHF vent fluids represent the waning stages of a hydrothermal system that involves hydrothermal alteration of an off-axis mafic intrusion and adjacent ultramafic wall rock at 200–300 °C. These temperature conditions optimize olivine hydrolysis reactions, which serve as a key pH constraint and H_2 generation mechanism, while relatively unaltered mafic rocks provide the noteworthy source of dissolved alkali metals. Such a model agrees well with genetic models of oceanic core complexes that point to preferential uplift of deeply emplaced gabbro intrusions relative to abyssal peridotite followed by periodic (10–100 kyr) off-axis magmatic intrusions (Ildefonse et al., 2007; Olive and Crone, 2018). The frequency of these intrusions and mode of emplacement provides an important control on the thermal regime of the massifs, including the depths and temperatures of hydrothermal circulation (Chen et al., 2022). At the initial stages of intrusion, high-temperature alteration of emplaced mafic intrusions, dikes, and sills leads to production of acidic hydrothermal fluids, leading to the observed amphibole + chlorite ± talc veining and Si-metasomatism of intruded ultramafic units. These initial fluids are expected to be generally similar to those collected at the Rainbow Vent Field and other acidic hydrothermal systems developed on oceanic core complexes, which are attributed to amphibolite + chlorite + talc equilibria (Seyfried et al., 2011) reminiscent of the amphibolite + chlorite ± talc veins and talc mineralization observed in Atlantis Massif drill cores (Früh-Green et al., 2018; Rouméjon et al., 2018; Liebmann et al., 2018; Whattam et al., 2022a, 2022b). Hydrothermal cooling and progressive penetration of circulating fluids eventually leads to reaction at lower (< 350 °C) temperatures and a switch from acidic to alkaline vent fluids. This shift in fluid pH would be accompanied by numerous other changes, including much decreased Fe-, sulfide-, and CO_2 concentrations, which are precipitated under alkaline, lower-temperature conditions. The depletion of all of these components is a well-recognized attribute of LCHF vent fluids.

Further evidence for the role of magmatic intrusions in driving the LCHF system is provided by the previously enigmatic observation that LCHF vent fluids are 2 % depleted in Cl relative to seawater (Seyfried et al., 2015). At the time, phase separation effects were ruled out because estimated reaction temperatures were insufficient to achieve phase separation at the proposed depths (Seyfried et al., 2015). However, with the recognition that LCHF vent fluids can be effectively reproduced by hydrothermal alteration of mafic rocks and peridotite at elevated fluid:rock ratios, we propose that this 2 % depletion reflects admixture of an (acidic) Cl-depleted vapor that forms in the immediate vicinity of a residual hot core of the mafic intrusion with alkaline, seawater-salinity fluid formed by reaction with solidified mafic rocks and peridotite at the proposed 200–300 °C reaction temperatures. Because the bulk of the hydrothermal fluid arises from lower-temperature reaction, the originally acidic vapor is effectively titrated, and Cl concentrations mix toward seawater values. Even at modest pressure, constrained by the subseafloor depth of the putative gabbro body, temperatures in excess of 450 °C are likely needed to account for the observed salinity depletions of the LCHF fluids—higher pressures leading to more saline vapors and accordingly a greater vapor-derived fraction of LCHF vent fluids.

Alternatively, it has been proposed that the observed Cl depletion reflects Cl uptake into serpentine during olivine hydrolysis (e.g., Seyfried et al., 2015). However, detailed mineralogical and $\delta^{37}Cl$ isotope studies of marine serpentinites indicate that the majority of Cl present in these samples occurs as interstitial water-soluble phases, such as halite or bischofite, the presence of which is indicative of highly concentrated saline pore water developed during effectively closed-system mineral hydration reactions (Sharp and Barnes, 2004; Barnes and Sharp, 2006). Results of peridotite serpentinization experiments likewise indicate that

fluid Cl concentrations increase during serpentinization (e.g., Seyfried et al., 2007), in contrast to the Cl depletion observed in LCHF vent fluids. Recognition that relatively unaltered off-axis mafic intrusions are an essential component of the LCHF system and that the chemical characteristics of LCHF vent fluids most clearly represent a temperature effect on the relative reactivities of plagioclase and olivine leads to two important conclusions. First, that oceanic core complexes can be expected to host geochemically diverse hydrothermal vent fields, which, in order of decreasing reaction temperature, include: (1) high-temperature acidic vent fields such as the Rainbow Vent Field, (2) higher-Si, lower H_2 vent fields such as the Von Damm Hydrothermal Field (McDermott, 2015), and (3) alkaline, H_2-rich vent fields such as LCHF. Second, that LCHF-type hydrothermal systems may not be common in the modern ocean, nor a direct analog for early-Earth or extraterrestrial hydrothermal systems. Distinct from the model of McCaig et al. (2007), which likewise proposes a genetic connection between Rainbow and Lost City vent fields, we emphasize the role of progressive cooling and hydrothermal reaction of discrete, episodic off-axis mafic intrusions, which has implications for vent field exploration. As an example of these processes, evidence for fluid evolution from high-temperature acidic fluids to lower-temperature alkaline fluids associated with intrusion of an oceanic core complex by MORB gabbro has also been reported in an Apennine ophiolite (Alt et al., 2018).

5.4. Implications for Hydrothermal Vent Exploration

Alkaline, H_2-rich hydrothermal vent fields conceptually similar to the LCHF have been identified as promising sites for prebiotic chemistry and early life evolution (Martin and Russell, 2007), supported by evidence from the LCHF for abiotic organic synthesis (Proskurowski et al., 2008; McDermott et al., 2015) and extant microbial communities dominated by metabolically ancient methanogenic archaea (Brazelton et al., 2006; Lang et al., 2018; Brazelton et al., 2022). Thus, the interpretation that LCHF vent fluids derive from peridotite serpentinization reactions (Kelley et al., 2001; 2005; Seyfried et al., 2015) has had a profound effect on the search for habitable early-Earth or extraterrestrial environments, motivating exploration of hydrothermally altered ultramafic rocks on Mars (Tutolo and Tosca, 2023), Europa, and Enceladus (Zolotov and Shock, 2004; Vance et al., 2007; Glein and Waite, 2020, McCollom et al., 2022).

In contrast, the model supported here suggests that vigorously venting alkaline H_2-rich vent systems as exemplified by the LCHF are more likely to be associated with mafic intrusions, which may themselves contain the necessary olivine, than with peridotite alone. Accordingly, exploration strategies targeting alkaline hydrothermal systems should prioritize identification of subaqueous heat sources. Furthermore, petrologic search criteria, especially remote sensing criteria, which are more likely to be optimized toward major rather than minor mineral phases, should be expanded to include mafic as well as ultramafic rock types.

In the modern-Earth ocean, H_2-rich, typically acidic, hydrothermal vents have been found along slow- and ultraslow spreading ridges (e.g., Batuyev et al., 1994; Charlou et al., 2002; Douville et al., 2002; German et al., 2010; Pedersen et al., 2010; McDermott et al., 2018; German et al., 2022), where crustal extension is accommodated by tectonic movements and episodic magmatic intrusions (Mutter and Karson, 1992; Dick et al., 2003). Previous interpretations of the LCHF have generally proposed that hydrothermal activity is driven by continuous processes such as exothermic chemical reaction (Kelley et al., 2005), tectonically driven deep fluid circulation (Titarenko and McCaig, 2017), or slot convection (Lowell, 2017). In contrast, our analyses suggest that the LCHF is the result of episodic, possibly discrete off-axis mafic intrusions and therefore represents a transient, waning stage of hydrothermal activity. Such a conclusion is in line with other investigations of hydrothermal activity along slow and ultraslow spreading ridges, which have led to renewed recognition of the importance of magmatic heat in driving hydrothermal systems. For example, a water-column survey of the Gakkel Ridge, the slowest spreading ridge system on Earth (full spreading rate = 6–13 mm/yr), identified hydrothermal plumes originating from 9 to 12 distinct hydrothermal plumes, all associated with volcanic centers (Edmonds et al., 2003; German et al., 2022). High-temperature vent systems on the Mid-Atlantic Ridge (Douville et al., 2002), Mid-Cayman Rise (German et al., 2010; McDermott et al., 2018), and Southwest Indian Ridge (Tao et al., 2012) are likewise associated with ongoing or recent magmatic activity.

Hydrothermal activity associated with discrete magmatic intrusions must likewise be discontinuous in nature and proceed according to a lifecycle ultimately governed by gradual cooling of the emplaced magma body. In the case of olivine-bearing rock types, such cooling leads to a dramatic change in fluid chemistry from acidic, metal-rich vent fluids at high ($> 350\ ^\circ C$) reaction temperatures to alkaline, metal-poor vent fluids at lower ($< 350\ ^\circ C$) reactions temperatures (Allen and Seyfried, 2003; Seyfried et al., 2010). With reference to known vent fields, we propose that emplacement of a mafic intrusion at a slow- or ultraslow spreading ridge initially leads to high-temperature water–rock reactions that produce acidic vent fluids, as currently observed at the Rainbow-, Ashadze-, Logatchev-, Niebelungen, Semenov, and Irinovskoe vent fields. As the intrusion cools, lower-temperature reactions produce alkaline vent fluids such as those at LCHF, possibly passing through a thermally and chemically intermediate stage represented by the Von Damm Hydrothermal Field. The revealing existence of Cl depleted vapors in LCHF vent fluids, however, provides evidence of a still active magmatic heat source. When magmatic heat is exhausted, weak low-temperature fluid flow may persist, as currently observed at the Old City Hydrothermal Field (Lecoeuvre et al., 2021). The Rainbow Massif, which hosts the inactive Ghost City and Clamstone sites (Lartaud et al., 2011) as well as the highly active Rainbow Vent Field (Douville et al., 2002), represents both ends of this lifecycle. Because the alkaline, H_2-rich vent fluids observed at LCHF occupy a narrow thermal window in the geologic evolution of hydrothermal activity associated with episodic off-axis mafic intrusions, we anticipate that such systems are likely to be rare in the modern ocean.

6. Conclusions

This study demonstrates the utility of stable K-isotope analyses in generating insights about processes underlying seafloor hydrothermal systems that could not otherwise be determined. Here, high-precision K-isotope measurements and analyses of K-isotope systematics indicate that LCHF vent fluids cannot be derived from hydrothermal alteration of mantle peridotite alone. Instead, we propose a two-stage reaction involving mafic and ultramafic rocks at 200–300 °C. We thus propose that LCHF represents a transient waning stage of hydrothermal circulation initially induced by an off-axis magmatic intrusion, although one still sufficiently hot to generate a vapor-phase fluid, the importance of which cannot be over-emphasized in terms of the temporal evolution of such systems, now, and throughout Earth history. We additionally propose that episodic magmatic intrusions along slow-spreading ridges will lead to a succession of hydrothermal vent fluids proceeding from acidic fluids produced at initial high reaction temperatures to alkaline fluids produced at lower reaction temperatures. In this context, the LCHF represents a particular stage in this evolutionary sequence rather than a quasi-ubiquitous class of alkaline hydrothermal vent inevitably produced by geologic uplift of ultramafic mantle rocks to the seafloor.

CRediT authorship contribution statement

Guy N. Evans: conceptualization, software, investigation, writing. **Soisiri Charin:** investigation, methodology, validation. **William E. Seyfried Jr.:** investigation, resources, writing, supervision, administration, funding acquisition. **Xinyuan Zheng:** conceptualization, investigations, methodology, resources, writing, supervision,

administration, funding acquisition.

Declaration of competing interest

The authors declare that they have no known competing financial interests or personal relationships that could have appeared to influence the work reported in this paper.

Data availability

Data are available through the Data Repository for the University of Minnesota (DRUM) at https://hdl.handle.net/11299/265196.

Acknowledgments

We gratefully acknowledge Frieder Klein as associate editor and three reviewers for their insightful comments and suggestions that led to improvements of this article. We additionally acknowledge the funding sources: NSF CAREER award 2238685 to XYZ, MGG-1736679 to WES.

Appendix A. Supplementary material

Supplementary materials include a Supplement containing details of elemental analyses and Sr-isotope-based estimates of water:rock ratios, MATLAB code used to calculate fluid:rock ratios based on K isotope systematics and a zipped folder containing GWB input, output and database files for thermodynamic models of fluid chemistry and alteration mineral assemblages predicted for reactions at 250 bar and 350 bar pressure. Supplementary material to this article can be found online at https://doi.org/10.1016/j.gca.2024.08.030.

References

Allen, D.E., Seyfried Jr, W.E., 2003. Compositional controls on vent fluids from ultramafic-hosted hydrothermal systems at mid-ocean ridges: An experimental study at 400 °C, 500 bars. Geochim. Cosmochim. Acta 67 (8), 1531–1542.

Allen, D.E., Seyfried Jr, W.E., 2004. Serpentinization and heat generation: constraints from Lost City and Rainbow hydrothermal systems. Geochim. Cosmochim. Acta 68 (6), 1347–1354.

Alt, J., Crispini, L., Gaggero, L., Levine, D., Lavagnino, G., Shanks, P., Gulbransen, C., 2018. Normal faulting and evolution of fluid discharge in a Jurassic seafloor ultramafic-hosted hydrothermal system. Geology 46 (6), 523–526.

Aquino, K.A., Früh-Green, G.L., Rickli, J., Bernasconi, S.M., Lang, S.Q., Lilley, M.D., Butterfield, D.A., 2022. Multi-stage evolution of the Lost City hydrothermal vent fluids. Geochim. Cosmochim. Acta 332, 239–262.

Awolayo, A.N., Tutolo, B.M., 2022. PyGeochemCalc: A Python package for geochemical thermodynamic calculations from ambient to deep Earth conditions. Chem. Geol. 606, 120984.

Barnes, J.D., Sharp, Z.D., 2006. A chlorine isotope study of DSDP/ODP serpentinized ultramafic rocks: insights into the serpentinization process. Chem. Geol. 228 (4), 246–265.

Batuyev, B.N., 1994. Massive sulfide deposits discovered at 14° 45'N, Mid-Atlantic Ridge. Bridge Newsletter 6, 6–10.

Beltenev, V.B., Ivanov, V.N., Sergeev, M.B., Rozhdestvenskaya, I.I., Samovarov, M.L., 2012. Results of prospecting works for base metal sulfides in the Atlantic Ocean in 2011 in the light of submitting the Russian application in ISA. Razved. Okhr. Nedr 8, 50–55.

Beltenev, V., Neschertov, A., Shilov, V., Ivanov, V., Shagin, A., Stepanova, T., Cherkashev, G., Batuev, B., Samavarov, M., Rozhdestvenskaya, I., Andreeva, I., Federov, I., Davydov, M., Romanova, A., Rumyantsev, A., Zaharov, V., Luneva, N., Artem'eva, O., 2003. New discoveries at 12°58'N, 44° 52'W, MAR: Professor Logatchev-22 cruise, initial results. InterRidge News 12 (1), 13–14.

Berndt, M.E., Allen, D.E., Seyfried Jr, W.E., 1996. Reduction of CO_2 during serpentinization of olivine at 300 C and 500 bar. Geology. 24 (4), 351–354.

Berndt, M. E., Seyfried Jr, W. E., Beck, J. W., 1988. Hydrothermal alteration processes at midocean ridges: experimental and theoretical constraints from Ca and Sr exchange reactions and Sr isotopic ratios. *J. Geophys. Res.: Solid Earth*, *93*(B5), 4573-4583.

Bethke, C. M., Yeakel, S., 2014. The geochemist's workbench. Release 10.0. GWB essentials guide. *Aqueous Solutions, LLC, Champaign, IL, 149p*.

Blackman, D. K., Ildefonse, B., John, B. E., Ohara, Y., Miller, D. J., Abe, N., Abratis, M., Andal, E, S., Andreani, M., Awaji, S., Beard, J. S., Brunelli, D., Charney, A. B., Christie, D. M., Collins, J., Delacour, A. G., Delius, H., Drouin, M., Einaudi, F., Escartín, J., Frost, B. R., Früh-Green, G., Fryer, P. B., Gee, J. S., Godard, M., Grimes, C. B., Halfpenny, A., Hansen, H. -E., Harris, A. C., Tamura, A. Hayman, N. W., Hellebrand, E., Hirose, T., Hirth, J. G., Ishimaru, K., Johnson, T. M., Karner, G. D., MacLeod, C. J., Maeda, J., Mason, O. U., McCaig, A. M., Michibayashi, K., Morris, A., Nakagawa, T., Nozaka, T., Rosner, M., Searle, R. C., Suhr, G., Tominaga, M., von der Handt, A., Yamasaki, T., Zhao, X., 2011. Drilling constraints on lithospheric accretion and evolution at Atlantis Massif, Mid-Atlantic Ridge 30 N. *J. Geophys. Res.: Solid Earth*, *116*(B7).

Blackman, D.K., Karson, J.A., Kelley, D.S., Cann, J.R., Früh-Green, G.L., Gee, J.S., Hurst, S.D., Joh, B., E., Morgan, J., Nooner, S. L., Ross, D. K., Schroeder, T. J., Williams, E. A, 2002. Geology of the Atlantis Massif (Mid-Atlantic Ridge, 30 N): Implications for the evolution of an ultramafic oceanic core complex. Marine Geophysical Researches 23, 443–469.

Blackman, D.K., Slagle, A., Guerin, G., Harding, A., 2014. Geophysical signatures of past and present hydration within a young oceanic core complex. Geophys. Res. Lett. 41 (4), 1179–1186.

Blackman, D. K., 2006. Proceedings of the Integrated Ocean Drilling Program, 304/305.

Boschi, C., Dini, A., Früh-Green, G.L., Kelley, D.S., 2008. Isotopic and element exchange during serpentinization and metasomatism at the Atlantis Massif (MAR 30 N): insights from B and Sr isotope data. Geochim. Cosmochim. Acta 72 (7), 1801–1823.

Boschi, C., Früh-Green, G. L., Delacour, A., Karson, J. A., Kelley, D. S., 2006. Mass transfer and fluid flow during detachment faulting and development of an oceanic core complex, Atlantis Massif (MAR 30 N). *Geochem., Geophys., Geosys.*, *7*(1).

Bowers, T. S., Taylor Jr, H. P., 1985. An integrated chemical and stable-isotope model of the origin of midocean ridge hot spring systems. *J. Geophys. Res.: Solid Earth*, *90* (B14), 12583-12606.

Brazelton, W.J., Schrenk, M.O., Kelley, D.S., Baross, J.A., 2006. Methane-and sulfur-metabolizing microbial communities dominate the Lost City hydrothermal field ecosystem. Applied and Environmental Microbiology 72 (9), 6257–6270.

Brazelton, W.J., McGonigle, J.M., Motamedi, S., Pendleton, H.L., Twing, K.I., Miller, B. C., Lowe, W.J., Lang, S.Q., 2022. Metabolic strategies shared by basement residents of the Lost City hydrothermal field. Applied and Environmental Microbiology 88 (17), e00929–e01022.

Canales, J. P., Tucholke, B. E., Xu, M., Collins, J. A., DuBois, D. L., 2008. Seismic evidence for large-scale compositional heterogeneity of oceanic core complexes. *Geochem., Geophys., Geosys.*, *9*(8).

Cann, J.R., Blackman, D.K., Smith, D.K., McAllister, E., Janssen, B., Mello, S., Avgerinos, E., Pascoe, A.R., Escartin, J., 1997. Corrugated slip surfaces formed at ridge–transform intersections on the Mid-Atlantic Ridge. Nature 385 (6614), 329–332.

Cannat, M., Fontaine, F., Escartín, J., 2010. Serpentinization and associated hydrogen and methane fluxes at slow spreading ridges, in: Rona, P. A., Devey, C. W., Dyment, J., Murton, B. J., (Eds.), *Diversity of hydrothermal systems on slow spreading ocean ridges*, American Geophysical Union, AGU Monograph Series, 188, 241-264.

Charlou, J.L., Donval, J.P., Fouquet, Y., Jean-Baptiste, P., Holm, N., 2002. Geochemistry of high H_2 and CH_4 vent fluids issuing from ultramafic rocks at the Rainbow hydrothermal field (36 14′ N, MAR). Chem. Geol. 191 (4), 345–359.

Chen, J., Olive, J. A., Cannat, M., 2022. Thermal regime of slow and ultraslow spreading ridges controlled by melt supply and modes of emplacement. *J. Geophys. Res.: Solid Earth*, *127*(4), e2021JB023715.

Debret, B., Beunon, H., Mattielli, N., Andreani, M., Da Costa, I.R., Escartin, J., 2018. Ore component mobility, transport and mineralization at mid-oceanic ridges: A stable isotopes (Zn, Cu and Fe) study of the Rainbow massif (Mid-Atlantic Ridge 36°14'N). Earth Planet. Sci. Lett. 503, 170–180.

Delacour, A., Früh-Green, G.L., Frank, M., Gutjahr, M., Kelley, D.S., 2008. Sr-and Nd-isotope geochemistry of the Atlantis Massif (30 N, MAR): implications for fluid fluxes and lithospheric heterogeneity. Chem. Geol. 254 (1–2), 19–35.

Devey, C.W., Lackschewitz, K.S., Baker, E., 2005. Hydrothermal and volcanic activity found on the southern Mid-Atlantic Ridge. Eos, Transactions American Geophysical Union 86 (22), 209–212.

Dick, H.J., Lin, J., Schouten, H., 2003. An ultraslow-spreading class of ocean ridge. Nature 426 (6965), 405–412.

Douville, E., Charlou, J.L., Oelkers, E.H., Bienvenu, P., Colon, C.J., Donval, J.P., Fouquet, Y., Prieur, d., Appriou, P, 2002. The rainbow vent fluids (36 14′ N, MAR): the influence of ultramafic rocks and phase separation on trace metal content in Mid-Atlantic Ridge hydrothermal fluids. Chem. Geol. 184 (1–2), 37–48.

Drouin, M., Godard, M., Ildefonse, B., Bruguier, O., Garrido, C.J., 2009. Geochemical and petrographic evidence for magmatic impregnation in the oceanic lithosphere at Atlantis Massif, Mid-Atlantic Ridge (IODP Hole U1309D, 30 N). Chem. Geol. 264 (1–4), 71–88.

Edmonds, H.N., Michael, P.J., Baker, E.T., Connelly, D.P., Snow, J.E., Langmuir, C.H., Dick, H.J.B., Mühe, R., German, C.R., Graham, D.W., 2003. Discovery of abundant hydrothermal venting on the ultraslow-spreading Gakkel ridge in the Arctic Ocean. Nature 421 (6920), 252–256.

Evans, G.N., Coogan, L.A., Kaçar, B., Seyfried Jr., W.E., 2023. Molybdenum in basalt-hosted seafloor hydrothermal systems: Experimental, theoretical, and field sampling approaches. Geochim. Cosmochim. Acta 353, 28–44.

Fouquet, Y., Barriga, F.J.A.S., Charlou, J.L., Elderfield, H., German, C.R., Ondreas, H., Parson, L., Radford-Knoery, J., Ribiero, R.J., Schultz, A., Apprioual, R., Cambon, P., Costa, I., Donval, J.-P., Douville, E., Ladure, J., Normand, A., Pelle, H., Ponsevera, E., 1998. FLORES diving cruise with Nautile near the Azores-First dives on the Rainbow field: hydrothermal seawater/mantle interaction. InterRidge News 7 (1), 24–28.

Foustoukos, D.I., Savov, I.P., Janecky, D.R., 2008. Chemical and isotopic constraints on water/rock interactions at the Lost City hydrothermal field, 30 N Mid-Atlantic Ridge. Geochim. Cosmochim. Acta 72 (22), 5457–5474.

Früh-Green, G.L., Orcutt, B.N., Green, S.L., Cotterill, C., 2017. Atlantis massif serpentinization and life. Proc, Intern. Ocean Discov. Prog., p. 357

Früh-Green, G.L., Orcutt, B.N., Rouméjon, S., Lilley, M.D., Morono, Y., Cotterill, C., Green, S., Escartin, J., John, B.E., McCaig, A.M., Cannat, M., Menez., B., Scharzenbach, E. M., Williams, M. J., Morgan, S., Lang, S. Q., Schrenk, M. O.,

Brazelton, W. J., Akizawa, N., Boschi, C., Dunkel, K. G., Quemenseur, M., Whattam, S. A., Mayhew, L., Harris, M., Bayracki, G., Behrmann, J. -H., Herrero-Bervera, E., Hesse, K., Liu, H-Q., Ratnayake, a. S., Twing, K., Weis, D., Zhao, R., Bilenker, L, 2018. Magmatism, serpentinization and life: Insights through drilling the Atlantis Massif (IODP Expedition 357). Lithos 323, 137–155.

Gale, A., Dalton, C. A., Langmuir, C. H., Su, Y., Schilling, J. G., 2013. The mean composition of ocean ridge basalts. *Geochem., Geophys., Geosys.*, *14*(3), 489-518.

Gallant, R. M., Von Damm, K. L., 2006. Geochemical controls on hydrothermal fluids from the Kairei and Edmond vent fields, 23–25 °S, Central Indian Ridge. *Geochem., Geophys., Geosys.*, *7*(6).

German, C.R., Bowen, A., Coleman, M.L., Honig, D.L., Huber, J.A., Jakuba, M.V., Kinsey, M.D., Leroy, S., McDermott, J.M., Mercier de Lepinay, B., Nakamura, K., Seewald, J.S., Smith, J.L., Sylva, S.P., Van Dover, C.L., Whitcomb, L.L., Yoerger, D. R., 2010. Diverse styles of submarine venting on the ultraslow spreading Mid-Cayman Rise. Proc. Nat. Acad. Sci. 107 (32), 14020–14025.

German, C.R., Reeves, E.P., Türke, A., Diehl, A., Albers, E., Bach, W., Purser, a., Ramalho, S. P., Suman, S., Mertens, C., Walter, M., Ramirez-Llodra, E., Schlindwein, V., Bünz, S., Boetius, A, 2022. Volcanically hosted venting with indications of ultramafic influence at Aurora hydrothermal field on Gakkel Ridge. Nat. Comm. 13 (1), 6517.

Glein, C. R., Waite, J. H., 2020. The carbonate geochemistry of Enceladus' ocean. *Geophys. Res. Lett.*, *47*(3), e2019GL085885.

Godard, M., Awaji, S., Hansen, H., Hellebrand, E., Brunelli, D., Johnson, K., Yamasaki, T., Maeda, J., Abratis, M., Christie, D., Kato, Y., Mariet, C., Rosner, M., 2009. Geochemistry of a long in-situ section of intrusive slow-spread oceanic lithosphere: Results from IODP Site U1309 (Atlantis Massif, 30 N Mid-Atlantic-Ridge). Earth Planet. Sci. Lett. 279 (1–2), 110–122.

Grozeva, N.G., Klein, F., Seewald, J.S., Sylva, S.P., 2017. Experimental study of carbonate formation in oceanic peridotite. Geochim. Cosmochim. Acta 199, 264–286.

Henig, A. S., Blackman, D. K., Harding, A. J., Canales, J. P., Kent, G. M., 2012. Downward continued multichannel seismic refraction analysis of Atlantis Massif oceanic core complex, 30° N, Mid-Atlantic Ridge. *Geochem., Geophys., Geosys.*, *13*(5).

Hille, M., Hu, Y., Huang, T.Y., Teng, F.Z., 2019. Homogeneous and heavy potassium isotopic composition of global oceans. Science Bulletin 64 (23), 1740–1742.

Hu, Y., Teng, F. Z., Helz, R. T., Chauvel, C., 2021. Potassium isotope fractionation during magmatic differentiation and the composition of the mantle. *J. Geophys.Res.: Solid Earth*, *126*(3), e2020JB021543.

Hulme, S. M., Wheat, C. G., 2019. Subseafloor fluid and chemical fluxes along a buried-basement ridge on the eastern flank of the Juan de Fuca Ridge. *Geochem., Geophys., Geosys.*, *20*(11), 4922-4938.

Ildefonse, B., Blackman, D., John, B.E., Ohara, Y., Miller, D.J., MacLeod, C.J., 2006. IODP Expeditions 304 305 characterize the lithology, structure, and alteration of an oceanic core complex. Scientific Drilling 3, 4–11.

Ildefonse, B., Blackman, D.K., John, B.E., Ohara, Y., Miller, D.J., MacLeod, C.J., 2007. Oceanic core complexes and crustal accretion at slow-spreading ridges. Geology. 35 (7), 623–626.

Janecky, D.R., Seyfried Jr., W.E., 1986. Hydrothermal serpentinization of peridotite within the oceanic crust: Experimental investigations of mineralogy and major element chemistry. Geochim. Cosmochim. Acta 50 (7), 1357–1378.

Karson, J. A., Früh-Green, G. L., Kelley, D. S., Williams, E. A., Yoerger, D. R., Jakuba, M., 2006. Detachment shear zone of the Atlantis Massif core complex, Mid-Atlantic Ridge, 30 N. *Geochem., Geophys., Geosys.*, *7*(6).

Kelley, D.S., Karson, J.A., Blackman, D.K., Früh-Green, G.L., Butterfield, D.A., Lilley, M. D., Olson, E.J., Schrenk., M. O., Roe, K. K., Lebon, G. T., Rivizzigno, P, 2001. AT3-60 Shipboard Party, An off-axis hydrothermal vent field near the Mid-Atlantic Ridge at 30 °N. Nature 412 (6843), 145–149.

Kelley, D.S., Karson, J.A., Früh-Green, G.L., Yoerger, D.R., Shank, T.M., Butterfield, D.A., Hayes, J.H., Schrenck, M.O., Olson., E. J., Proskurowski, G., Jakuba, M., Bradley, A., Larson, B., Ludwig, K., Glickson, D., Buckman, K., Bradley, A. S., Brazelton, W. J., Roe, K., Elend, M. J., Delacour, A., Bernasconi, S, M., Lilley, M, D., Baross, J, A., Summons, R. E., Sylva, S. P, 2005. A serpentinite-hosted ecosystem: the Lost City hydrothermal field. Science 307 (5714), 1428–1434.

Krasnov, S.G., Cherkashev, G.A., Stepanova, T.V., Batuyev, B.N., Krotov, A.G., Malin, B. V., Maslov, M.N., Markov, V.F., Poroshina, I.M., Samavarov, M., s., Ashadze, A. M., Lazareva, L. I., Ermolayev, I. K, 1995. Detailed geological studies of hydrothermal fields in the North Atlantic. Geological Society, London, Special Publications 87 (1), 43–64.

Lang, S.Q., Butterfield, D.A., Schulte, M., Kelley, D.S., Lilley, M.D., 2010. Elevated concentrations of formate, acetate and dissolved organic carbon found at the Lost City hydrothermal field. Geochim. Cosmochim. Acta 74 (3), 941–952.

Lang, S.Q., Früh-Green, G.L., Bernasconi, S.M., Brazelton, W.J., Schrenk, M.O., McGonigle, J.M., 2018. Deeply-sourced formate fuels sulfate reducers but not methanogens at Lost City hydrothermal field. Scientific Reports 8 (1), 755.

Lang, S.Q., Lilley, M.D., Baumberger, T., Früh-Green, G.L., Walker, S.L., Brazelton, W.J., Kelley, D.S., Elend, M., Butterfield, D.A., Mau, A.J., 2021. Extensive decentralized hydrogen export from the Atlantis Massif. Geology. 49 (7), 851–856.

Lartaud, F., Dd Rafélis, M., Oliver, G., Krylova, E., Dyment, J., Ildefonse, B., Thibaud, R., Gente, P., Hoisé, E., Meisterzheim, A-L., Fouquet, Y., Gaill, F., Le Bris, N., 2010. Fossil clams from a serpentinite-hosted sedimented vent field near the active smoker complex Rainbow, MAR, 36°13' N: Insight into the biogeography of vent fauna. *Geochem., Geophys., Geosys.*, *11*(8).

Lartaud, F., Little, C.T., de Rafelis, M., Bayon, G., Dyment, J., Ildefonse, B., Gressier, V., Fouquet, Y., Gaill, F., Le Bris, N., 2011. Fossil evidence for serpentinization fluids fueling chemosynthetic assemblages. Proc. Nat. Acad. Sci. 108 (19), 7698–7703.

Lecoeuvre, A., Ménez, B., Cannat, M., Chavagnac, V., Gérard, E., 2021. Microbial ecology of the newly discovered serpentinite-hosted Old City hydrothermal field (southwest Indian ridge). The ISME Journal 15 (3), 818–832.

Li, W., Coogan, L.A., Wang, K., Takahashi, Y., Shakouri, M., Hu, Y., Liu, X.M., 2024. Hydrothermal origin of heavy potassium isotope compositions in altered oceanic crust: Implications for tracing the elemental cycle. Earth Planet. Sci. Lett. 625, 118448.

Liebmann, J., Schwarzenbach, E. M., Früh-Green, G. L., Boschi, C., Rouméjon, S., Strauss, H., Wiechart, U., John, T., 2018. Tracking Water-Rock Interaction at the Atlantis Massif (MAR, 30° N) Using Sulfur Geochemistry. *Geochem., Geophys., Geosys.*, *19* (11), 4561-4583.

Lissenberg et al., (in press) Science.

Liu, H., Xue, Y.Y., Zhang, G., Sun, W.D., Tian, Z., Tuller-Ross, B., Wang, K., 2021. Potassium isotopic composition of low-temperature altered oceanic crust and its impact on the global K cycle. Geochim. Cosmochim. Acta 311, 59–73.

Lowell, R.P., 2017. A fault-driven circulation model for the Lost City hydrothermal field. Geophys. Res. Lett. 44 (6), 2703–2709.

MacLeod, C.J., Searle, R.C., Murton, B.J., Casey, J.F., Mallows, C., Unsworth, S.C., Achenback, K.I., Harris, M., 2009. Life cycle of oceanic core complexes. Earth Planet. Sci. Lett. 287 (3–4), 333–344.

Magenheim, A. J., Spivack, A. J., Alt, J. C., Bayhurst, G., Chan, L. H., Zuleger, E., Gieskes, J. M., 1995. 13. Borehole fluid chemistry in hole 504B, LEG 137: formation water or in-situ reaction?. In *Proceedings of the Ocean Drilling Program, Scientific Results* (Vol. 137, No. 140, pp. 141-52).

Martin, W., Russell, M. J., 2007. On the origin of biochemistry at an alkaline hydrothermal vent. *Phil. Trans. Royal Society B: Biological Sciences*, *362*(1486), 1887-1926.

McCaig, A.M., Cliff, R.A., Escartin, J., Fallick, A.E., MacLeod, C.J., 2007. Oceanic detachment faults focus very large volumes of black smoker fluids. Geology 35 (10), 935–938.

McCaig, A., Lang, S.Q., Blum, P., and the Expedition 399 Scientists, 2024. Expedition 399 Preliminary Report: Building Blocks of Life, Atlantis Massif. International Ocean Discovery Program.

McCollom, T.M., Klein, F., Robbins, M., Moskowitz, B., Berquó, T.S., Jöns, N., Bach, W., Templeton, A., 2016. Temperature trends for reaction rates, hydrogen generation, and partitioning of iron during experimental serpentinization of olivine. Geochim. Cosmochim. Acta 181, 175–200.

McCollom, T.M., Klein, F., Moskowitz, B., Berquó, T.S., Bach, W., Templeton, A.S., 2020. Hydrogen generation and iron partitioning during experimental serpentinization of an olivine–pyroxene mixture. Geochim. Cosmochim. Acta 282, 55–75.

McCollom, T.M., Klein, F., Moskowitz, B., Solheid, P., 2022. Experimental serpentinization of iron-rich olivine (hortonolite): Implications for hydrogen generation and secondary mineralization on Mars and icy moons. Geochim. Cosmochim. Acta 335, 98–110.

McDermott, J.M., Seewald, J.S., German, C.R., Sylva, S.P., 2015. Pathways for abiotic organic synthesis at submarine hydrothermal fields. Proc. Nat. Acad. Sci. 112 (25), 7668–7672.

McDermott, J.M., Sylva, S.P., Ono, S., German, C.R., Seewald, J.S., 2018. Geochemistry of fluids from Earth's deepest ridge-crest hot-springs: Piccard hydrothermal field. Mid-Cayman Rise. *Geochim. Cosmochim. Acta* 228, 95–118.

McDermott, J. M., 2015. *Geochemistry of deep-sea hydrothermal vent fluids from the Mid-Cayman Rise, Caribbean Sea* (Doctoral dissertation, Massachusetts Institute of Technology).

Melchert, B., Devey, C.W., German, C.R., Lackschewitz, K.S., Seifert, R., Walter, M., Mertens, C., Yoerger, D.R., Baker, E.T., Paulick, H., Nakamura, K., 2008. First evidence for high-temperature off-axis venting of deep crustal/mantle heat: The Nibelungen hydrothermal field, southern Mid-Atlantic Ridge. Earth Planet. Sci. Lett. 275 (1–2), 61–69.

Mutter, J.C., Karson, J.A., 1992. Structural processes at slow-spreading ridges. Science 257 (5070), 627–634.

Olive, J. A., Crone, T. J., 2018. Smoke without fire: How long can thermal cracking sustain hydrothermal circulation in the absence of magmatic heat?. *J. Geophys. Res.: Solid Earth*, *123*(6), 4561-4581.

Pedersen, R.B., Rapp, H.T., Thorseth, I.H., Lilley, M.D., Barriga, F.J., Baumberger, T., Flesland, K., Fonseca, R., Früh-Green, G., Jorgensen, S.L., 2010. Discovery of a black smoker vent field and vent fauna at the Arctic Mid-Ocean Ridge. Nat. Comm. 1 (1), 126.

Proskurowski, G., Lilley, M.D., Seewald, J.S., Früh-Green, G.L., Olson, E.J., Lupton, J.E., Sylva, S.P., Kelley, D.S., 2008. Abiogenic hydrocarbon production at Lost City hydrothermal field. Science 319 (5863), 604–607.

Ramos, D.P.S., Nielsen, S.G., Coogan, L.A., Scheuermann, P.P., Seyfried Jr, W.E., Higgins, J.A., 2022. The effect of high-temperature alteration of oceanic crust on the potassium isotopic composition of seawater. Geochim. Cosmochim. Acta 339, 1–11.

Reeves, E.P., Seewald, J.S., Sylva, S.P., 2012. Hydrogen isotope exchange between n-alkanes and water under hydrothermal conditions. Geochim. Cosmochim. Acta 77, 582–599.

Rouméjon, S., Früh-Green, G.L., Orcutt, B.N., Expedition, I.O.D.P., 357 Science Party, 2018. Alteration heterogeneities in peridotites exhumed on the southern wall of the Atlantis Massif (IODP Expedition 357). J. Petrol. 59 (7), 1329–1358.

Ryan, W.B.F., Carbotte, S.M., Coplan, J.O., O'Hara, S., Melkonian, A., Arko, R., Weissel, R.A., Ferrini, V., Goodwillie, A., Nitsche, F., Bonczkowski, J., Zemsky, R., 2009. Global Multi-Resolution Topography synthesis. Geochem, Geophys. Geosys., p. 10

Schmidt, K., Koschinsky, A., Garbe-Schönberg, D., de Carvalho, L.M., Seifert, R., 2007. Geochemistry of hydrothermal fluids from the ultramafic-hosted Logatchev

hydrothermal field, 15 °N on the Mid-Atlantic Ridge: Temporal and spatial investigation. Chem. Geol. 242 (1–2), 1–21.
Schmidt, K., Garbe-Schönberg, D., Koschinsky, A., Strauss, H., Jost, C.L., Klevenz, V., Königer, P., 2011. Fluid elemental and stable isotope composition of the Nibelungen hydrothermal field (8° 18′ S, Mid-Atlantic Ridge): Constraints on fluid–rock interaction in heterogeneous lithosphere. Chem. Geol. 280 (1–2), 1–18.
Seewald, J.S., Doherty, K.W., Hammar, T.R., Liberatore, S.P., 2002. A new gas-tight isobaric sampler for hydrothermal fluids. Deep Sea Research Part i: Oceanographic Research Papers 49 (1), 189–196.
Seyfried Jr, W.E., Bischoff, J.L., 1979. Low temperature basalt alteration by sea water: an experimental study at 70 °C and 150 °C. Geochim. Cosmochim. Acta 43 (12), 1937–1947.
Seyfried Jr, W.E., Dibble Jr, W.E., 1980. Seawater-peridotite interaction at 300 °C and 500 bars: implications for the origin of oceanic serpentinites. Geochim. Cosmochim. Acta 44 (2), 309–321.
Seyfried Jr, W. E., Pester, N., Fu, Q., 2010. Phase equilibria controls on the chemistry of vent fluids from hydrothermal systems on slow spreading ridges: Reactivity of plagioclase and olivine solid solutions and the pH-silica connection. , in: Rona, P. A., Devey, C. W., Dyment, J., Murton, B. J., (Eds.), *Diversity of hydrothermal systems on slow spreading ocean ridges*, American Geophysical Union, AGU Monograph Series, 188, 297-320.
Seyfried Jr, W.E., Foustoukos, D.I., Fu, Q., 2007. Redox evolution and mass transfer during serpentinization: An experimental and theoretical study at 200 °C, 500 bar with implications for ultramafic-hosted hydrothermal systems at Mid-Ocean Ridges. Geochim. Cosmochim. Acta 71 (15), 3872–3886.
Seyfried Jr, W.E., Pester, N.J., Ding, K., Rough, M., 2011. Vent fluid chemistry of the Rainbow hydrothermal system (36 °N, MAR): Phase equilibria and in situ pH controls on subseafloor alteration processes. Geochim. Cosmochim. Acta 75 (6), 1574–1593.
Seyfried Jr, W.E., Pester, N.J., Tutolo, B.M., Ding, K., 2015. The Lost City hydrothermal system: Constraints imposed by vent fluid chemistry and reaction path models on subseafloor heat and mass transfer processes. Geochim. Cosmochim. Acta 163, 59–79.
Sharp, Z.D., Barnes, J.D., 2004. Water-soluble chlorides in massive seafloor serpentinites: a source of chloride in subduction zones. Earth Planet. Sci. Lett. 226 (1–2), 243–254.
Tao, C., Lin, J., Guo, S., Chen, Y.J., Wu, G., Han, X., German, C.R., Yoerger, D.R., Zhou, N., Li, H., Su, X., Zhu, J., 2012. DY115-19 (Legs 1–2) and DY115-20 (Legs 4–7) Science Parties, First active hydrothermal vents on an ultraslow-spreading center: Southwest Indian Ridge. Geology 40 (1), 47–50.
Titarenko, S.S., McCaig, A.M., 2016. Modelling the Lost City hydrothermal field: influence of topography and permeability structure. Geofluids 16 (2), 314–328.
Tucholke, B. E., Lin, J., Kleinrock, M. C., 1998. Megamullions and mullion structure defining oceanic metamorphic core complexes on the Mid-Atlantic Ridge. *J. Geophys. Res.: Solid Earth*, 103(B5), 9857-9866.
Tuller-Ross, B., Savage, P.S., Chen, H., Wang, K., 2019a. Potassium isotope fractionation during magmatic differentiation of basalt to rhyolite. Chem. Geol. 525, 37–45.
Tuller-Ross, B., Marty, B., Chen, H., Kelley, K.A., Lee, H., Wang, K., 2019b. Potassium isotope systematics of oceanic basalts. Geochim. Cosmochim. Acta 259, 144–154.
Tutolo, B. M., Tosca, N. J., 2023. Observational constraints on the process and products of Martian serpentinization. Sci. Adv., 9(5), eadd8472.
Vance, S., Harnmeijer, J., Kimura, J., Hussmann, H., DeMartin, B., Brown, J.M., 2007. Hydrothermal systems in small ocean planets. Astrobiology 7 (6), 987–1005.
Von Damm, K.L., Edmond, J.M., Grant, B., Measures, C.I., Walden, B., Weiss, R.F., 1985. Chemistry of submarine hydrothermal solutions at 21° N. East Pacific Rise. *Geochim. Cosmochim. Acta* 49 (11), 2197–2220.
Wang, K., Ionov, D.A., 2023. Potassium isotope evidence for slab-derived fluids in the sub-arc mantle. Earth Planet. Sci. Lett. 619, 118315.
Wang, K., Jacobsen, S.B., 2016. An estimate of the Bulk Silicate Earth potassium isotopic composition based on MC-ICPMS measurements of basalts. Geochim. Cosmochim. Acta 178, 223–232.
Wang, K., Close, H.G., Tuller-Ross, B., Chen, H., 2020. Global average potassium isotope composition of modern seawater. ACS Earth and Space Chemistry 4 (7), 1010–1017.
Wang, D.T., Reeves, E.P., McDermott, J.M., Seewald, J.S., Ono, S., 2018. Clumped isotopologue constraints on the origin of methane at seafloor hot springs. Geochim. Cosmochim. Acta 223, 141–158.
Whattam, S.A., De Hoog, J.C., Leybourne, M.I., Khedr, M.Z., 2022. Link between melt-impregnation and metamorphism of Atlantis Massif peridotite (IODP Expedition 357). Contributions to Mineralogy and Petrology 177 (11), 106.
Whattam, S. A., Früh-Green, G. L., Cannat, M., De Hoog, J. C., Schwarzenbach, E. M., Escartín, J., John, b. E., Leybourne, M. I., Williams, M. J., Rouméjon, S., Akizawa, N., Boschi, C., Harris, M., Wenzel, K., McCaig, A., Weis, D., Bilenker, L., 2022a. Geochemistry of serpentinized and multiphase altered Atlantis Massif peridotites (IODP Expedition 357): Petrogenesis and discrimination of melt-rock vs. fluid-rock processes. *Chem. Geol.*, 594, 120681.
Wheat, C.G., Mottl, M.J., 2000. Composition of pore and spring waters from Baby Bare: Global implications of geochemical fluxes from a ridge flank hydrothermal system. Geochim. Cosmochim. Acta 64 (4), 629–642.
Zheng, X.Y., Chen, X.Y., Ding, W., Zhang, Y., Charin, S., Gérard, Y., 2022a. High precision analysis of stable potassium (K) isotopes by the collision cell MC-ICP-MS "Sapphire" and a correction method for concentration mismatch. J. Analytical Atomic Spectrometry 37 (6), 1273–1287.
Zheng, X.Y., Beard, B.L., Neuman, M., Fahnestock, M.F., Bryce, J.G., Johnson, C.M., 2022b. Stable potassium (K) isotope characteristics at mid-ocean ridge hydrothermal vents and its implications for the global K cycle. Earth Planet. Sci. Lett. 593, 117653.
Zolotov, M. Y., Shock, E. L., 2004. A model for low-temperature biogeochemistry of sulfur, carbon, and iron on Europa. *J. Geophys. Res.: Planets*, *109*(E6).